Engineering Failure Analysis 66 (2016) 577–595

Contents lists available at ScienceDirect

Engineering Failure Analysis

journal homepage: www.elsevier.com/locate/engfailanal

Review

# A review on diffusion modelling in hydrogen related failures of metals

A. Díaz *, J.M. Alegre, I.I. Cuesta

*Structural Integrity Group, Escuela Politécnica Superior, Avda. Cantabria s/n, 09006 Burgos, Spain*

ARTICLE INFO

*Article history:*
Received 16 February 2016
Received in revised form 15 April 2016
Accepted 14 May 2016
Available online 06 April 2016

*Keywords:*
Hydrogen embrittlement
Multiscale modelling
Hydrogen diffusion

ABSTRACT

Modelling of hydrogen embrittlement in order to prevent engineering failures requires a characterization of transport phenomena in the bulk metallic as a first step. Interstitial solid state diffusion can be described as a random phenomenon, however there will be also some drift forces biasing this behaviour so a modification in Fick's laws is needed. The potential energy landscape of the metal lattice characterizes the influence of imposed fields and microstructural defects in transport kinetics. Thus, considering the chemical potential as a driving force, the physical basis of diffusion will be translated into continuum equations. Finally the two-level models that take into account lattice and trapping sites for hydrogen will be reviewed.



**Contents**



* Corresponding author.
*E-mail address:* adportugal@ubu.es (A. Díaz).

http://dx.doi.org/10.1016/j.engfailanal.2016.05.019
1350-6307/

## 1. Introduction

Hydrogen embrittlement is a common phenomenon which degrades metals [1–7]. A reduction in mechanical properties of metals and alloys occurs due to the inclusion of hydrogen as an impurity. The inserted atom is considerably smaller than the crystal atom so these phenomena fall under the category of interstitial solid solutions, in contrast to substitutional diffusion. This problem was documented over a century ago as a problem associated with the corrosion due to electrochemical reduction of hydrogen in aqueous media and also due to the gaseous hydrogen storage.

In literature there are plenty examples of hydrogen degradation associated with corrosion phenomena. For example, numerous failures attributed to hydrogen assisted cracking have been documented in pipelines transporting natural gas or oil [8]. Such petrochemical products typically contain $H_2S$ which promote an aggressive environment in which hydrogen is produced and diffuses through the metal causing embrittlement. For this reason, API pipeline X grades steels has been thoroughly investigated and tested in hydrogen environments (e.g. X42 [9]; X60, X80 and X100 [10]).

Additionally, cathodic protection, sometimes used in order to avoid corrosion, for example in buried pipes or in marine environments, results in hydrogen production which can produce unexpected failures [11,12].

Similarly, hydrogen absorption might occur in parts that have been plated, e.g. Tanner documented failures of cadmium plated head cap screws during service and attributed them to hydrogen embrittlement [13].

Welding processes may also introduce significant amounts of hydrogen from materials in the electrode coating, in the flux or in the shielding gas, as well as from the moist environment [14]. This hydrogen insertion added to the usual presence of residual stresses in the weld frequently causes Hydrogen Assisted Cracking [15].

In recent decades, since hydrogen has been proposed as a promising energy carrier, the interest in the interaction between hydrogen and different types of materials for hydrogen storage has increased.

Several methods of storing hydrogen have been [16]: liquid hydrogen at cryogenic temperatures, by physisorption, as a metal hydride and in gaseous state at high pressures. The last is the least expensive and consist in storing $H_2$ in pressure vessels made of alloys or composite materials. However, although $H_2$ containers have been built for more than a century, embrittlement of the used alloys still is a problem. The explosion of some iron bottles storing gaseous hydrogen in an airship in 1894 [17] might be regarded as one of the first failure cases of hydrogen containers documented. Hydrogen assisted cracking produced the release of hydrogen, as a result supplying an explosive gas mixture.

Also in the space industry hydrogen embrittlement has been a concern since failures have been documented in high-pressure hydrogen storage vessels at NASA facilities from 70s [18].

Revisiting this and other failure cases shows the importance of integrity assessment and hydrogen embrittlement prognosis in storage systems.

Despite the efforts, a full understanding of the phenomenon has not yet been achieved and selection of suitable components for hydrogen service simply discriminates between especially susceptible alloys (high strength steels, and nickel alloys) and alloys hardly affected (austenitic stainless steels and aluminum alloys), as the Standard ANSI/CSA CHMC 1-2014 defines [19]. Such distinction has an empirical basis but lacks of a consistent microstructural and physical explanation. Therefore, assessment of hydrogen embrittlement must move towards a physical-based numerical modelling of the metal-hydrogen system.

Usually, the interaction of metal-hydrogen is divided into two parts: transport phenomena (absorption and diffusion) and damage mechanisms. Both phenomena are related, but in this paper only the mathematical models that try to establish constitutive equations of diffusion are reviewed. The ultimate aim of diffusion modelling is to obtain concentration profiles to predict where and how the fracture will begin or where the more severe damage will occur. In any case, a consistent theory of diffusion and the influence of the stress-strain fields on it will not only produce more accurate concentration profiles, but it will result in a better understanding of the damage micro-mechanisms.

The objective of this review is to develop a simplified continuum level model from the general physics fundamentals. Firstly, the multiscale and multidisciplinary character of materials science is underlined and in particular that of hydrogen embrittlement. Later, mass transport is physically explained and the interstitial diffusion mechanism is explained as a random motion at the atomic level.

Next, the importance of characterizing the energy landscape of the metal lattice is shown and what the factors are that influence the energy state of an inserted hydrogen atom. Spatial variations in such free potential energy are discussed as a driving force. This leads to defining and characterizing the chemical potential as a continuum function. In order to consider all the effects

in a single driving force, one must know how the chemical potential changes with the variation of concentration and stress state. These functions can be found using thermodynamic properties and statistical physics. Chemical equilibrium or, alternatively, kinetic relationships between components or between sites is also discussed.

Then, through appropriate simplifications, the physical concepts exposed are related to the continuous diffusion models that are most commonly used in finite element simulations. These are models that consider only two types of sites for hydrogen: interstitial sites and microstructural traps.

Finally, the coupled nature of diffusion is briefly reviewed from a numerical point of view. The equations presented are related to damage micromechanisms involved. In this sense, hydrogen embrittlement is explained by a great number of theories but two of them are the most developed: HEDE (Hydrogen enhanced decohesion) in which hydrogen expands the matrix and so the cohesion and the fracture energy are reduced [20–22] and HELP (Hydrogen locally enhanced plasticity) in which hydrogen favours the mobility of dislocations which implies local plasticity even if there is a macroscopically brittle failure [23–25]. Furthermore, in some metals, dissolved atomic hydrogen can establish bonds with the metal element. Thus, the resulting hydrides can also produce embrittlement [25,26] but these considerations are beyond the scope of this review where only the situations in which hydrogen is in a solution are considered.

## 2. Multiscale approach

In materials science there is often, unfortunately, a gap between the different approaches modelling the same fact; nevertheless, in recent years the need of a multiscale approach in modelling has been emphasised [27,28]. Diffusion and hydrogen embrittlement are not exceptions.

Regarding the hydrogen transport, diffusion has usually been a phenomenological science based on the laws of Fick and Arrhenius. Because both classical theories and quantum physics agree in these behaviours, researchers can find unprofitable to follow a quantum approach [29].

However, due to the nature of the metals, quantum physics and solid state physics have become increasingly important in the field of metallurgy and in the prediction of properties of such materials. In addition, with regard to hydrogen diffusion, quantum effects are not always negligible because the small size and mass of the hydrogen atom causes that it cannot be treated as a classical particle [30].

For example, a quantum phenomenon that can alter the prognosis made by classical physics in terms of mass transport is tunnelling [31–33]. Diffusion in this case is not thermally activated and thus an Arrhenius-based approach would be wrong.

At the atomic level, metallic bonding properties vary due to the insertion of hydrogen. Besides, at microscopic scale, the interaction of hydrogen with certain defects such as dislocations must be also considered.

In this sense, the presumed absence of a single mechanism to explain hydrogen embrittlement is remarkable: models that may seem contradictory at the continuum level, such as decohesion (HEDE) versus localized plasticity (HELP) should be explained at the microscopic or even atomic level.

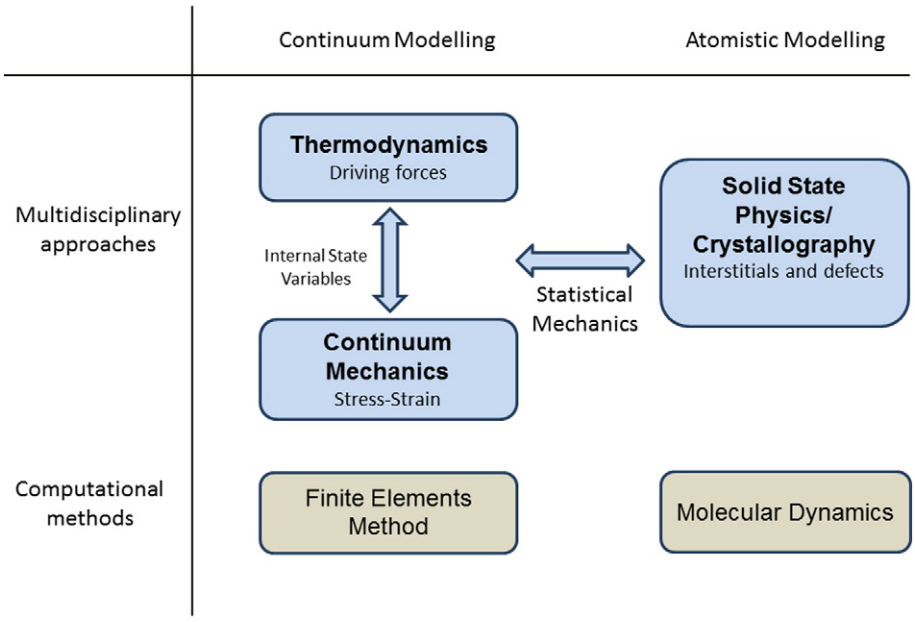


**Fig. 1.** Multiscale approaches (blue) and its respective computational methods (brown). Boxes on the left correspond to a continuum scale while boxes on the right are related to the atomic scale.

Therefore, even if diffusion can be described by a continuum description in a first approximation, the micro-mechanisms of damage must count with the interaction of hydrogen with crystal defects.

Furthermore, the amplitude of scales is not only dimensional but also temporary. Diffusion involves jumps occurring in femtoseconds, but the evolution of the whole system can last for months or years and affect the durability or integrity of a component in its service life.

There is also a gap between scales in the computational methods used to simulate these phenomena. Continuum mechanics use finite element simulation as the main tool. Its handicap arises when it is required to model small regions like crack tips where, as noted, atomic phenomena are important. Finite element methods are also limited when the material is not homogeneous and there are defects altering the behaviour, as it occurs in the diffusion of hydrogen.

On the other hand, the atomistic approach utilizes molecular dynamics whose disadvantage is that only small regions and short time windows can be modelled [30]. Still, this computational tool is useful for finding properties of metals and their interaction with hydrogen. In the context of transport phenomena, due to the random walk nature of diffusion, the Monte Carlo method is usually applied [34,35].

The present review consists in the following conceptual scheme: an understanding of the diffusion phenomenon as a random jump at atomic level that, due to the interstitial solution properties, is translated into driving forces associated with macroscopic thermodynamic magnitudes. This means that, although the review aims at putting the focus on the modelling of continuous, previously the basics of diffusion will be presented in connection with solid state physics (Fig. 1). It is also shown how statistical mechanics serve as a bridge between the two scales.

It is noteworthy that not only the interstitial transport must be described; hydrogen entry at surfaces plays a key role. When adsorption/absorption occurs in aqueous media, an electrochemical approach should be considered. Thus, in many processes of interest in the degradation of metals by hydrogen, electrochemistry is an indispensable science [36–38].

## 3. Diffusion phenomena

Basically, diffusion is a mass transport from one region to another caused by concentration gradients. The flux of particles in a mixture tends to a dispersion of the components until the complete mixing is achieved. This fact was first observed in fluids and later in solids [39]. Chronologically, the Fick's phenomenological approach of preceded the study of molecular diffusion, but in the subsequent development of models the opposite path is followed.

### 3.1. Einstein equation for Brownian motion

In his work on Brownian movement [40], Albert Einstein presented a kinetic theory explaining the randomness in the motion of particles in suspension observed by Robert Brown. A relation between the diffusion coefficient $D$, the temperature $T$ and the fluid viscosity is found: it is called Stokes-Einstein relation. More generically, a mobility coefficient $B$ is defined that in the case of Brownian motion would depend on the viscosity and particle size:

$$D = Bk_BT. \tag{1}$$

Such generic equation is called Einstein-Smoluchowski relation. Although supposedly Brownian motion only refers to fluids, an analogy with crystalline solids can be made since diffusion has also the random walk as a basis [41].

However, the causes of this random motion are different: classical Brownian motion is produced by collisions of pollen particles with fluid molecules whereas interstitial solid diffusion is caused by the vibrations of the interstitial impurity and its random jump to a neighbour site.

### 3.2. Diffusion as a random walk

In order to prove the randomness of diffusion, it is supposed a certain hydrogen mass $M$ deposited at $x = 0$ in a unidimensional path. Initially, it is assumed that each hydrogen atom has the same opportunities to make a jump to the left than to the right. The atoms that make many more steps towards one side than towards the other side will move away very much from the origin. However, most of atoms make approximately the same number of hops to the right than to the left. This leads to the hypothesis that the distribution will approach, as the number of steps increases, to a normal distribution. The randomness leading to such distribution is what is known as Gaussian White Noise. In fact, the differential equation that represents Fick's second law can be easily solved [42] obtaining:

$$C(x,t) = \frac{M}{2\sqrt{\pi \mathrm{Dt}}} \exp\left(-\frac{x^2}{4Dt}\right). \tag{2}$$

It is proved that $C(x,t)/M$ approaches a normal distribution centered in the origin, i.e. with a mean value of $\mu = 0$, and with a variance of $\sigma^2 = 2Dt$. Therefore Fick's law is compatible with a random movement. Actually, the diffusion equations are a particularization of the Fokker-Planck equation governing the evolution of a stochastic event such as Brownian motion [43] or, in this

case, the interstitial solid diffusion. Drift forces are also included in the Fokker-Planck equation [44].This deviation is discussed in Section 3.5.

It is important to highlight, that the standard deviation depends on time: the more time elapses the distribution will be "extended". Knowing the properties of a normal distribution, $\sigma^2$ is the expected value of the square of the distance to the mean. Therefore, on average, the square of the displacement $\varepsilon$ of an atom is expected to be [40]:

$$\varepsilon^2 = 2Dt. \tag{3}$$

The expression is only valid for the one-dimensional diffusion. Generically, instead of a factor of 2, a $\gamma$ coefficient that takes into account the geometry can be included. For instance, for the three-dimensional case, $\gamma = 6$.

While the movement of a single particle in a given time may thus be described with the concept of random motion, it is not possible to tell in which direction it will move in that time [42]. However, considering no longer a particle but a large set of particles distributed in a region, random motion will result statistically in a net flux from regions of high concentration to regions of low concentration; this fact occurs simply because there are more molecules in the area of high concentration.

### 3.3. Landscape of potential energies

From this perspective, diffusion is the balance of hops between the different sites where the hydrogen atom can stay. In the diffusion equations position is a continuous magnitude, but metals have a crystalline structure so those sites correspond to the unoccupied spaces at atomic level and the equilibrium position of an atom is actually a discrete variable.

As a result of the interatomic attractions generated by the metal lattice, sites where hydrogen tends to stay correspond to areas of low potential energy. Interatomic potentials are usually treated as a two-body problem; however, an impurity in a metal crystal is a many-body problem. In order to solve this difficulty, there are different approaches that derive analytic potentials from semi-empirical quantum-mechanics arguments.

Among them there is the Embedded Atom Method (EAM) developed by Daw and Baskes that allows to find the interatomic potential and to characterize the influence of defects and impurities in metals [45,46].

Some works [47,48] perform a multiscale modelling considering two regions: an interior zone where Quantum Mechanics (QM) calculations are done including Density Functional Theory (DFT) and an outer region where Molecular Mechanics (MM) calculations are performed with the EAM. An interaction energy must be included in order to couple the two scales (QM/MM). This procedure is a tool for obtaining preference sites and energy distributions.

Thus, analyzing the diffusion in certain orientation $x$, the potential trace $V(x)$ will have some well points where the hydrogen atom can be placed and saddle points to be overcome in the hop between neighbour sites (Fig. 2).

Diffusion is a thermally activated process, i.e. energy is needed to overcome the saddle, at most of the temperatures of interest in industrial and technological processes. However, as discussed in Section 2, an effect called quantum tunnelling has been found in which the hydrogen atom can move to an adjacent site through the barrier with less energy than expected. For most systems tunnelling is dominant only at low temperature [49]; nonetheless Katzarov et al. [50] demonstrate, using the path integral theory, that for iron quantum effects play a crucial role in hydrogen diffusion even at ambient temperature. For example, they found that binding free energies at a vacancy increase significantly when quantum effects are considered.

When there is an ideal crystal lattice, the depths of the wells will be repeated periodically according to a pattern dependent on the orientation. However, the potential distribution might be modified in two ways [39]. Firstly, when other potential field $\phi(x)$ is imposed:

$$V(x) = V_0(x) + \phi(x) \tag{4}$$

where $V_0(x)$ is the potential trace of the perfect lattice, i.e. without defects. For example, the stress state can be regarded as a potential field superimposed.

Secondly, when there are defects in the metal lattice: these places are broader and therefore the hydrogen present in them is less attracted; thus, the well point is deeper and the retention of the hydrogen atom is stronger. Hydrogen may be in different

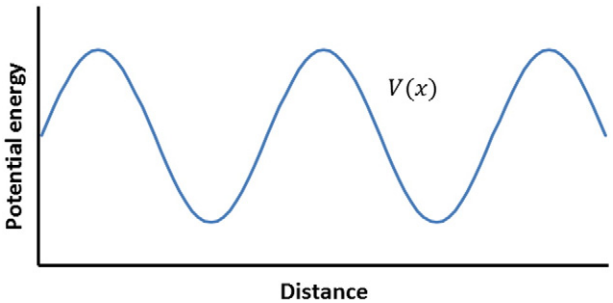


**Fig. 2.** Potential energy of a metal lattice along a certain $x$ direction.

lattice imperfections (e.g. inclusions, vacancies, dislocations, grain boundaries, second phases…) called microstructural traps [51]. The two main effects, as it will be seen in the following sections, are an increase in apparent solubility and a decrease in the apparent diffusivity [52].

When the potential trace is not uniform, the jump is biased towards directions of lower potential energy and thus it is not completely random. Actually, during the interstitial diffusion metal atoms move locally distorting the matrix, and therefore, each jump is never a complete stochastic event independent from the previous ones. In order to expect this independence, the matrix relaxation should be much faster than the time it takes a hop [53].

Following Kirchheim's work [54], a way of characterizing the state of a crystal imperfection is to describe the energy distribution. The potential wells correspond to the energy states $E$ in Fig. 3. Degeneracy of each state, $g(E)$, i.e., the number of times it is repeated on the total, may range from perfect crystal to amorphous state. In the first case, it is called one-level system since all potential wells have the same energy $E_0$. One kind of trap can be added with energy $E_t$ less than $E_0$; in this two-level system degeneracy of each level obviously depends on the concentration of traps. The extreme case is the amorphous state; although it is difficult to represent the distribution of defects, one can consider that degeneracy follows a Gaussian distribution, being the most probable energy state that of the ideal interstitial site.

In order to characterize the energy levels associated with different type of traps, there are different experimental techniques: one of the most used is Thermal Desorption Spectroscopy (TDS) [55,56] in which trapping energies are closely related to the temperature at which the rate of desorbed hydrogen is greater. Isothermal methods such as electrochemical permeation might also be used to find the energies associated with traps if a number of tests at different temperatures are made [57].

Such techniques have their limitations and with them it is challenging to obtain accurate values of binding energies for each type of trap because in the same specimen simultaneous effects of different traps occur [58]. Besides, by a well potential it is only possible to characterize the ideal vacancies or substitutional impurities. Most of the real traps have instead an associated distribution of energy wells and saddle points. Therefore, comparison of the experimental values with atomistic calculations (e.g. semi-empirical potential in the above-mentioned EAM) will be crucial for better energy characterization of the traps in each specific situation.

Energy distributions have been can be calculated by the EAM for different systems, e.g. for hydrogen in body-centered-cubic iron [59]. In this work of Wen et al., the obtained binding energies of dislocations and vacancies are in agreement with experimental values.

Grain boundaries (GB) are particularly complex because they not only act as trapping sites but they constitute accelerated diffusion paths or short-circuits [1]. However, knowledge and energy characterization of both phenomena are still limited.

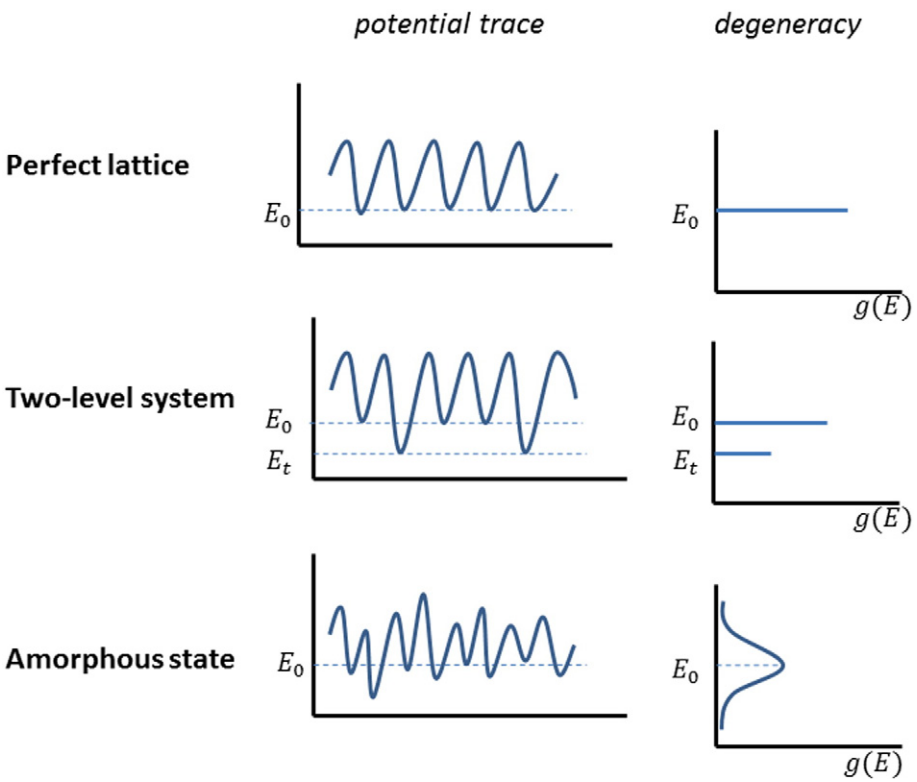


**Fig. 3.** Potential energy distribution and degeneracy of the well points in different configurations [54].

In nickel grain boundaries, Oudriss et al. studied these double effect [60] and concluded that trapping phenomena are predominant in GB in which there is a large density of dislocations and vacancies, whereas in the high-angle random boundaries hydrogen diffusion is accelerated [57].

Furthermore, the influence of hydrogen on grain boundary decohesion plays a fundamental role in intergranular fracture modelling [61].

### 3.4. Transition rate

Considering the metal lattice as a discrete space of sites, each jump is the step of a random walk with a length equal to the distance $a$ between two adjacent well points. In addition, the frequency of jump, i.e. the transition rate, will be the inverse magnitude of the time elapsed in a single step: $\Gamma = 1/t$. Starting from here, it is possible to reach numeric expressions of the diffusion coefficient.

#### 3.4.1. Hop between equal sites

When all sites are equal, i.e. matrix without defects or one-level system, and there is no interaction between interstitial hydrogen atoms because the concentration is very low and all neighbour sites are empty, a single jumping frequency can be defined by means of an Arrhenius law. The exponential term indicates the probability of thermal energy exceeding the diffusion barrier; in other words, a thermally-activated jump with $E_a$ is considered:

$$\Gamma = \Gamma_0 \exp\left(-\frac{E_a}{k_B T}\right). \tag{5}$$

The pre-exponential factor $\Gamma_0$ depends on the vibration frequency of the hydrogen atom, sometimes taken as the Debye frequency within the metal lattice and hence a quantum problem that is not reviewed here. This fact is related with tunnelling or delocalization. Therefore, deviation from the expected $-T^{-1}$ dependence of diffusion coefficient occurs at low temperatures [2]. Wimmer et al. obtain temperature-dependent diffusion coefficients in nickel from ab initio computations considering all vibrational terms [62]. The pre-exponential factor is also greatly isotope dependent [63].

The activation energy of a single hop is the difference between the well point and the saddle point that should be overcome in the direction of the jump. Most times, its value is fitted by empirical values of the diffusion coefficient. However, there exist elastic models able to calculate the diffusion barrier assuming a lattice elastic expansion [64]. However, with ε equal to the interatomic distance $a$:

$$D = \frac{1}{\gamma} a^2 \Gamma_0 \exp\left(-\frac{E_a}{k_B T}\right). \tag{6}$$

An Arrhenius type expression is obtained for $D$:

$$D = D_0 \exp\left(-\frac{E_a}{k_B T}\right). \tag{7}$$

#### 3.4.2. Hop between different sites

More generically, following Toribio and Kharin's work [65], it must be assumed that the jump occurs between different sites and even that the neighbour sites may already be occupied. The kinetics of mass exchange between two adjacent places, for instance A and B (Fig 4), can be described by the frequency $\Gamma_{A\to B}$ in which the hop from A to B occurs:

$$\Gamma_{A\to B} = \Omega_{A\to B} Y_B. \tag{8}$$

It is equal to the frequency $\Omega_{A\to B}$ in which the jump is attempted, multiplied by the probability that the jump is effective $Y_B$. The first term depends on the vibration frequency $\omega_{0A}$ of the particle in A and the activation energy $E_{A\to B}$ acting as a barrier between A and B:

$$\Omega_{A\to B} = \omega_{0A} \exp\left(-\frac{E_{A\to B}}{k_B T}\right). \tag{9}$$

The probability that the jump is effective $Y_B$ is equal to the probability of finding a B-type site $N_B$ / $N$ multiplied by the probability that it is empty $(1 - \theta_B)$. Where $N_B$ is the number of B-type sites; $N$ the total sites and $\theta_B$ the occupancy of this kind of sites. Numerically:

$$Y_B = \frac{N_B}{N}(1-\theta_B). \tag{10}$$

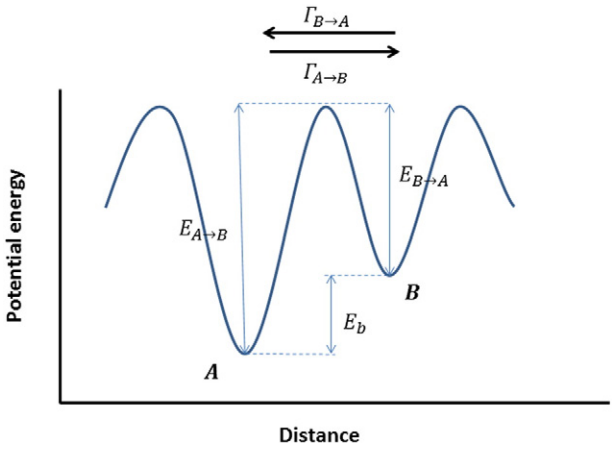


**Fig. 4.** Hop between two different sites A y B.

In these cases where there are two states the transition rate is not symmetrical and thus it will be an activation energy in each direction. The difference between both is called binding energy $E_b$ and characterizes each trap in relation with interstitial ideal sites. It is an inherently negative energy [66]. Because the transition rate is asymmetrical, the diffusion coefficient is specific for each pair. In addition, each hydrogen trap may be classified as reversible or irreversible depending on the activation energy needed to remove hydrogen from there.

### 3.5. Driving force and flux

In classical physics, a force is any magnitude capable of modifying the momentum of a particle or system. Knowing that in the fluids there is an analogy between the Transport Phenomena [67], i.e. momentum transfer, heat transfer and mass transfer, a force will also represent any agent capable of modifying the amount of energy or matter.

Momentum transfer has as driving force in a fluid the velocity gradient, which constitutes Newton's law relating the shear stress with such gradient and through the a coefficient called viscosity.

Analogically, there is the Fourier's law for heat transfer and Fick's law for mass diffusion. Focusing on diffusion, Fick's law assumes that the flux $J_i$ of particles of a component $i$ is proportional to the concentration gradient $\nabla C_i$. This proportionality allows defining the diffusivity or diffusion coefficient $D$ with units of type $m^2/s$. The negative sign indicates that transport is produced from high to low concentrations:

$$J_i = -D\nabla C_i. \tag{11}$$

Exchange of matter will happen until thermodynamic equilibrium is reached. This equilibrium is characterized by the absence of variations in different thermodynamic quantities. This condition does not always mean an absence of concentration gradients [68]. Onsager uses this fact to include the diffusion in the context of non-equilibrium thermodynamics [69,70]:

$$J_i = \sum_j L_{ij} F_j \tag{12}$$

where the component $i$ suffers a flux due to the different driving forces $F_j$. The matrix $L_{ij}$ contains the corresponding coefficients. Moreover, each driving force defines a scalar potential in the classical form:

$$F_j = -\nabla V_j. \tag{13}$$

In other words, the thermodynamic equilibrium may be defined as the absence of gradients on the potential of these forces. Usually, the driving forces are caused by variations in chemical potential $\mu_k$ of the components, in temperature T, in pressure P, and in other external potentials. For example, transport due to temperature gradients is called Soret effect or thermophoresis; osmosis is explained by the pressure gradient; or if the external potential is due to electrostatic forces, the expression obtained is the Nernst-Planck equation.

When several of these processes occur at the same time, in order to consider a less complex approach, it is taken into account that all driving forces can be reduced into gradients of chemical potential [71]. Thus, a flux of particles of component $i$ will be

created:

$$J_i = -\sum_k L_{ik}\nabla\mu_k. \tag{14}$$

When there is a multicomponent solution, the terms $k \neq i$ are designated as cross coefficients because they weight the influence of a component in the transport of the other.

A different approach consist in establishing that hydrogen flux is equal to the contribution of all the jumps ($\Gamma_{A\rightarrow B}$) passing through a particular surface. Using Fourier series, flux vector can be expressed at a given point [65]. This approach is more physical-based, but it is mathematically more complex than the phenomenological Onsager expression.

As noted, Fick's laws have a random distribution as numerical solution. This occurs when the only driving force is the concentration gradient. However, when the jump is not completely random, diffusion deviates from Fick's first law. This deviation can be described by a drift flux that is equal to the concentration multiplied by a quantity called drift velocity $v_j$, which is always associated with a driving force. It is assumed that there is only one component and thereby the subscript $i$ is removed:

$$J = -D\nabla C + v_j C \tag{15}$$

$$J = J_{random} + J_{drift}. \tag{16}$$

Following Teorell's formula, a relation between the velocity and the driving force is obtained through the associated mobility $B$ defined above.

$$v_j = BF_j. \tag{17}$$

Although drift velocity and drift flux were initially defined for drag forces occurring in fluids due to advection, i.e., due to the bulk transport of the media, it is also applicable in rigid solids considering other phenomena that cause deviation of random motion. In addition, this double flux term also serves to explain the Kirkendall effect [72].

Nevertheless, the approach based on the Eq. (14) allows to include both random effects and the deviation from them in the chemical potential as the only driving force. In this case, the flux is:

$$J = BCF = -\frac{D}{k_B T} C\nabla\mu \tag{18}$$

where the mobility is considered as expressed before. It could be shown how, for dilute solutions, substituting the value of the chemical potential as a function of concentration $\mu = \mu(C)$ Fick's first law is finally obtained.

## 4. Interstitial solid solutions

For the purpose of modelling the continuum, it must be found an accurate function of the chemical potential $\mu$. Then, a flux tending to equalize the chemical potentials until equilibrium is established.

There is a different thermodynamic approach that explains the random phenomena like Brownian motion considering that the main driving force is an entropy gradient [73]. As a conclusion drawn in Section 3.2, random motion of a certain mass tends to a normal distribution in unidimensional diffusion; in this probabilistic context, the normal distribution maximizes entropy. Consequently, both approaches must be equivalent.

### 4.1. Chemical potential

As noted, hydrogen atoms tend to stay in places of low potential free energy. From fundamental thermodynamic relations the chemical potential is defined as a molar free energy. Considering the Helmholtz free energy:

$$\mu_i = \left(\frac{\partial F}{\partial n_i}\right)_{T,V,n_{j\neq i}} \tag{19}$$

but the most common conditions in engineering are those of constant pressure and temperature. In that case the Gibbs free energy is used:

$$\mu_i = \left(\frac{\partial G}{\partial n_i}\right)_{P,T,n_{j\neq i}}. \tag{20}$$

As seen in Section 3.3, the potential energy landscape characterizes diffusion at the atomic level. Making the necessary corrections, microscopic properties of the lattice should be translated into macroscopic features (thermodynamic potentials). The tool that bridges the gap between both scales is provided by statistical mechanics.

Alternatively, through an atomic approach, Venturini et al. [74] define a particle chemical potential that may vary from particle to particle, thus it is not a uniform field. In such a case, driving forces and linear kinetics are considered discrete.

In this review, a continuum model is pursued so the main objective is to find a relationship between chemical activity expressed by the chemical potential and concentration, or equivalently, between chemical potential and occupancy.

*4.1.1. Statistical mechanics*

Entropy can be divided into a configurational part $S^c$, dependent on the "order" of the particles, and a non-configurational part $S^{nc}$. Configurational entropy follows Boltzmann law depending on the number of possible microstates $W$:

$$S^c = k_B \ln W. \tag{21}$$

Possible microstates are calculated by means of combinatory as a function of the number of particles $n$ and the number of possible sites $N$:

$$W = \frac{N!}{n!(N-n)!}. \tag{22}$$

Using, as it is usually done in statistical physics, Stirling's approximation, and an expression for the chemical potential is obtained [75]. Defining a dimensionless concentration called occupancy $\theta = n/N$:

$$\mu = \mu^{nc} + k_B T \ln\left(\frac{\theta}{1-\theta}\right). \tag{23}$$

If only the configurational entropy is considered, the model is called quasi-regular solution [76–78]. In this case, $\mu^{nc} = \mu^0$ is the molar enthalpy.

The next step is to take into account the interaction energy between pairs of atoms [79]: solute-site (H-S), solute-solute (H-H) and site-site (S-S). The total energy $E_k$ is the sum over all possible pairs. In that term the coordination number of interstitial sites is also included, depending on the type of cell [78]. Because there is an energetic degeneracy dependent on the configuration of the sites, the canonical ensemble is used, whose partition function $Z$ is:

$$Z = \sum_k g(E_K) \exp\left(-\frac{E_k}{k_B T}\right) \tag{24}$$

where the summation is made over each of the possible configurations $k$ and $g(E_K)$ is the degeneracy of each one. From this partition function, it can be found the Helmholtz free energy $F$:

$$F = -k_B T \ln Z. \tag{25}$$

There are two possibilities to calculate the partition function: zeroth order or first order treatment. In the first case it is considered that the atoms are randomly distributed in the interstitial sites so the sum of all states is replaced by a single degenerate state [80].

Actually, each interstitial solute atom restricts to a number of neighbour sites to be occupied. It is what is called quasi-chemical or first-order treatment [81]. In this approach, therefore, the entropy is not completely random. Now it is not possible to suppose a single degenerate state and the expression for degeneracy will be much more complex.

In both cases, however, there is a term independent on occupancy, $\mu^0$; another term associated with the number of possible microstates and finally a more or less extensive sequence of terms that depend on configuration $k$, on occupancy and on the interaction energy between hydrogen atoms $\varepsilon_h$:

$$\mu = \mu^0 + k_B T \ln\left(\frac{\theta}{1-\theta}\right) + f(k, \theta, \varepsilon_h). \tag{26}$$

A similar result is given by Christensen et al. [82] for the chemical potential of hydrogen in Palladium. Performing a thermodynamic analysis, available sites are considered in contact with an hydrogen reservoir [83,84].

*4.1.2. Fermi-Dirac distribution*

Hydrogen in a metal lattice follows Fermi-Dirac statistics because each energy state can be occupied only by an atom and therefore an analogy with the Pauli exclusion principle can be established. The probability that the $E_i$ level is occupied by a

hydrogen atom corresponds to the Fermi-Dirac distribution:

$$p_i = \frac{1}{1 + \exp\left(\frac{E_i - \mu}{k_B T}\right)}. \tag{27}$$

Equivalence between the chemical potential and the Fermi energy is assumed, although this is physically arguably [68]. The total occupancy will be:

$$\theta = \sum_i p_i g_i \tag{28}$$

where is $g_i$ the degeneracy of the energy state $E_i$, i.e. the density of site energies (DOSE) [85]. For an interstitial solid solution, being $N_i$ the total number of sites of type $i$, degeneracy means the normalized number of such sites:

$$g_i = \frac{N_i}{\sum N_i}. \tag{29}$$

If the energy levels are very close, occupancy and degeneracy can be expressed in a continuous manner:

$$\theta = \int_{-\infty}^{+\infty} \frac{g(E)}{1 + \exp\left(\frac{E - \mu}{k_B T}\right)} dE. \tag{30}$$

Therefore, from the Fermi-Dirac distribution and considering an expression of $g(E)$ it is possible to find the relationship between the occupancy and the chemical potential. The energy $E$ corresponds to the well points of the potential energy trace (Fig. 3).

Degeneracy has a different expression depending on whether one considers the perfect crystal, with certain defects or completely amorphous. There will be considered only extreme cases.

In the former case, a lattice without defects represents a completely degenerate state in which the distribution of sites follows the Dirac delta function [85]. The potential well is constant and equal to $E_0$.

$$g(E) = \delta(E - E_0). \tag{31}$$

Solving the corresponding integral (substituting Eq. (31) in (30)) and isolating the chemical potential, a similar expression is obtained where the term $\mu^0$ is equivalent to the energy of a potential well in the ideal matrix, $E_0$.

$$\mu = E_0 + k_B T \ln\left(\frac{\theta}{1 - \theta}\right). \tag{32}$$

For the latter case, the amorphous state, it is almost impossible to know the real distribution of defects and therefore the energy states distribution. Nevertheless, the amorphous state can be characterized as a deviation from the perfect crystal, i.e. with a mean value of $E_0$, following a normal distribution. Kirchheim [85] makes some simplifications in order to solve the integral and obtains for high temperatures and low concentrations:

$$\mu = E_0 - \frac{\sigma^2}{4 k_B T} + k_B T \ln\theta. \tag{33}$$

This expression tends to that of an ideal dilute solution ideal. The less irregular the crystal is (less deviation $\sigma^2$ from perfect lattice) the more ideal behaviour will have.

*4.1.3. Corrections*

As it was said in Section 3.3, potential energy trace can be derived from ab initio calculations based on solid state physics and quantum physics. However, the potential free energy of the system includes not only the lattice energy generated by the interatomic forces; vibrational and thermal effects must also be taken into account [86].

Therefore, when theoretical calculations of the chemical potential are compared with experimental results, two corrections should be introduced. The first correction is made by a phonon term or zero-point energy [87,88]. The second one is a correction due to the thermal electronic excitations [82].

### 4.2. Chemical activity

Chemical activity can be defined through the chemical potential:

$$\mu = \mu^0 + k_B T \ln a. \tag{34}$$

In this expression the chemical potential in a reference state $\mu^0$ corresponds to that of an activity equal to unity. Taking into consideration the forms of the chemical potential previously found, Henry's law and ideal behaviour are satisfied only for a dilute solution, i.e. $\theta \ll 1$.

Interaction effects between hydrogen atoms, non-configurational entropy excess and corrections by zero point energy and thermal excitations will be neglected hereinafter. And therefore, the chemical potential of a component $i$ (disregarding the stress state) will be:

$$\mu_i = \mu_i^0 + k_B T \ln \frac{\theta_i}{1-\theta_i}. \tag{35}$$

### 4.3. Equilibrium between sites

As said in Sections 3.3 and 3.4, there are various kinds of sites that can be seen as two different species. An exchange of matter between them, characterized by its energy relationship, is established. In a physicochemical approach, reaction between the hydrogen atoms ($H$) and the empty sites ($V$) of each state is assumed and therefore a law of mass action can be used [54]

$$H_A + V_B \rightleftarrows V_A + H_B. \tag{36}$$

When the reaction, that is, the exchange between A and B reaches equilibrium, a constant can be defined. Concentrations of empty and filled sites are here expressed in terms of the number of particles $n_i$ and the number of each type of site $N_i$:

$$K_{AB} = \frac{N_A - n_a}{N_B - n_B} \cdot \frac{n_B}{n_A}. \tag{37}$$

Expressed in terms of occupancy, $\theta_i = n_i/N_i$, Oriani's equilibrium [89] equation is obtained:

$$\frac{\theta_B}{1-\theta_B} = \frac{\theta_A}{1-\theta_A} K_{AB}. \tag{38}$$

The value of the equilibrium constant follows an Arrhenius law. This can be proved because in equilibrium between both species, their chemical potentials are equal. Therefore, with Eqs. (35) and (38) and imposing $\mu_A = \mu_B$:

$$K_{AB} = \exp\left(-\frac{\mu_B^0 - \mu_A^0}{k_B T}\right). \tag{39}$$

The difference between the potential in the standard state of both species can be seen as the enthalpy of formation of a reaction. In the context of diffusion affected by microstructural traps, this enthalpy is called the binding energy between the two sites: $E_b = \mu_B^0 - \mu_A^0$.

### 4.4. Stress state

Aiming at describing the evolution of the metal-hydrogen system, a thermodynamically consistent approach is necessary. It must take into account the balance (momentum, mass, energy) and the irreversibility of processes (dissipation and entropy) [90,91]. However, because this review focuses on transport models, only the possible influences of the stress state in the chemical potential are considered since this function represents the diffusion driving force.

In a lattice subjected to a traction stress state, the sites will be wider and hence the chemical potential will be lower. In different thermodynamic studies on stressed solids [92] it has been found:

$$\mu(\sigma_h) = \mu(\sigma_h = 0) - \sigma_h \overline{V}_H. \tag{40}$$

This means that the energy of interaction of hydrogen atoms with the stress field only depends on the diagonal terms of the stress tensor, $\sigma_h = \frac{1}{3}(\sigma_{11} + \sigma_{22} + \sigma_{33})$ and on the hydrogen partial molar volume $V_H$.

Here, only spherical distortion is considered. However, depending on the type of lattice there will be a greater or lesser anisotropy that causes non-symmetrical distortion [2]. In this case, the distortion is tetragonal and the off-diagonal stress terms are also important [93].

Interaction energy can also be calculated for a dislocation stress field interacting with an hydrogen atoms atmosphere [94,95]. This approach is fundamental in localized plasticity theories.

## 5. Two-level continuum model

With the aim of implementing a transport model in a finite element code, usually some simplifications are made. Thus, models that consider two types of sites are reviewed: lattice sites (subscript L) and trapping sites (subscript T). Therefore, it is a two-level model with the energy degeneracy shown schematically in Fig. 3 and all the lattice defects have the same binding energy. This is an idealization since there always are various types of traps in any metallic bulk. To extend the equations presented below for a model with more than one type of traps, the concentration of each kind of trap and their respective exchange kinetics equation must be introduced in the global mass balance [96–99].

Another simplification is to consider that all the saddle points have the same energy for the entire crystal. Therefore, a single activation energy is considered for interstitial diffusion $D_L$. Furthermore, this diffusivity is considered independent of concentration.

For convenience, hereinafter the more usual nomenclature in bibliography will be used. Energies are usually expressed per mol so the universal constant R is included. In addition, the occupation $\theta_i$ in each kind of site $i$ represents the relationship between the hydrogen concentration $C_i$ and the concentration $N_i$ of this type of site.

### 5.1. Interstitial flux

It is assumed, by definition, that traps are isolated from each other [90]. Thus $J_T = 0$ and only the interstitial flux is considered. Another interpretation [65] consists of neglecting flux between traps only if the jump between the two places is unlikely: when there are few traps or when excessive energy is required; in this case need not be considered isolated traps. Anyway, taking the interstitial flux (18), the total hydrogen flux is:

$$J = -\frac{D_L}{RT} C_L \nabla \mu_L. \tag{41}$$

This means that only interstitial diffusion is considered and the trapping influence is taken into account as a reaction between the two species.

Assuming $J_T = 0$ is a problematic simplification even though most of the numerical simulations in literature include it. In situations where many dislocations (for example in a crack tip due to the high level of plasticity) or in grain boundaries, there will be a large accumulation of trapping sites and therefore traps cannot be considered isolated. Simulations that take into account such fluxes in balance equations should be implemented in the future.

### 5.2. Chemical potential

Despite being the chemical potential gradient which governs diffusion, equations are traditionally expressed in terms of a more familiar physical variable: concentration. The simplification made here is to consider a dilute solution, i.e., low occupancy: $\theta_L \ll 1$. Thus, with (35) and (49) the chemical potential is:

$$\mu_L = \mu_L^0 + RT \ln \theta_L - \sigma_h \overline{V}_H. \tag{42}$$

Substituting Eq. (41) into (42) and operating, flux is obtained as a concentration function:

$$J = -D_L \nabla C_L + \frac{D_L}{RT} C_L \overline{V}_H \nabla \sigma_h. \tag{43}$$

It can be observed how, analogically to (15), (16) and (17), a random term and a drift flux have been obtained. The drift force is here the hydrostatic stress gradient.

### 5.3. Mass balance

Mass conservation implies that the variation of hydrogen concentration in the total volume must be equal to the flux through the surface containing it. Numerically:

$$\frac{\partial}{\partial t} \int_V (C_L + C_T) dV + \int_S J_L \cdot n \cdot \mathrm{d}S = 0. \tag{44}$$

Substituting (43) in (44) and using the divergence theorem, this balance represents a modified form of the second Fick's law.

$$\frac{\partial C_T}{\partial t}+\frac{\partial C_L}{\partial t}-\nabla\cdot(D_L\nabla C_L)+\nabla\cdot\left(\frac{D_L C_L \overline{V}_H}{RT}\nabla\sigma_h\right)=0. \tag{45}$$

This constitutive equation of diffusion must be solved by a numerical method such as the finite element method. To do this, it must be assumed a relationship between $C_L$and $C_T$. Different models present a correspondent meaning of the term $\partial C_T/\partial t$ quantifying the kinetics of exchange between interstitial sites and traps. All models reviewed are isothermal, i.e., there are no temporal or spatial temperature variations.

### 5.4. Trapping influence

Depending on the considered relationship between traps and interstices, a different numerical expansion of $\partial C_T/\partial t$ is obtained.

#### 5.4.1. Effective diffusivity

One of the first attempts, if not the first, to develop a finite element simulation of a two-level diffusion was made by Sofronis and McMeeking [66]. The general transport Eq. (45) can be rewritten:

$$\left(\frac{\partial C_T}{\partial C_L}+1\right)\frac{\partial C_L}{\partial t}-\nabla\cdot(D_L\nabla C_L)+\nabla\cdot\left(\frac{D_L C_L \overline{V}_H}{RT}\nabla\sigma_h\right)=0. \tag{46}$$

It is possible to define an effective diffusion coefficient representing the delay in diffusion produced by trapping:

$$D_{eff}=D_L\frac{1}{1+\partial C_T/\partial C_L}. \tag{47}$$

Finally, the general equation used by Sofronis and McMeeking has the form:

$$\frac{D_L}{D_{eff}}\frac{\partial C_L}{\partial t}=\nabla\cdot(D_L\nabla C_L)+\nabla\cdot\left(\frac{D_L C_L \overline{V}_H}{RT}\nabla\sigma_h\right). \tag{48}$$

In their work, Oriani's equilibrium is assumed. Deriving from (38) and with $\theta_L \ll 1$:

$$D_{eff}=D_L\frac{C_L}{C_L+C_T(1-\theta_T)}. \tag{49}$$

#### 5.4.2. Plastic strain influence

From the previous model, Krom et al. [100] consider the plastic strain rate. Applying the chain rule, an additional term is included:

$$\frac{\partial C_T}{\partial t}=\frac{\partial C_T}{\partial C_L}\frac{\partial C_L}{\partial t}+\frac{\partial C_T}{\partial N_T}\frac{dN_T}{d\varepsilon_p}\frac{\partial \varepsilon_p}{\partial t}. \tag{50}$$

Oriani's equilibrium is again assumed obtaining:

$$\frac{\partial C_T}{\partial t}=\frac{C_T(1-\theta_T)}{C_L}\frac{\partial C_L}{\partial t}+\theta_T\frac{dN_T}{d\varepsilon_p}\frac{\partial \varepsilon_p}{\partial t}. \tag{51}$$

The number of traps $N_T$ is not a characteristic value of the matrix and is very difficult to determine because of the large variety of microstructural defects that can be included under this category. However, various investigations have shown that the trap population is associated with dislocation density and depends on the level of plastic strain.

Despite the usual employment of expressions relating $N_T$ with $\varepsilon_P$, it should be noted that this is an important simplification: the number of traps depends not only on dislocations as there will be other types of traps: grain boundaries, vacancies, inclusions, etc.

In any case, one option is to obtain empirical relationships for $N_T - \varepsilon_P$ by means of diffusion and permeation tests [101–103]. A commonly used result is the obtained by Kumnick and Johnson [103] by permeation tests in alpha iron with different levels of equivalent plastic strain. Their results are fitted into the following expression [66]:

$$\log N_T = 23.26 - 2.33 \exp\left(-5.5\varepsilon_p\right). \tag{52}$$

It is also possible to assume a trap for each atomic plane intersected by a dislocation. Sofronis et al. [52,104] calculate the number of traps from the dislocation density $\rho$ (m/m$^3$), and the lattice parameter $a$ (m):

$$N_T = \sqrt{2}\rho/a. \tag{53}$$

This approach requires an empirical or semi-empirical expression for the variation of dislocation density with plastic deformation.

It should be noted here the possible consequence of Strain Gradient Plasticity theories that distinguish between statistically stored dislocations and geometrically necessary dislocations. Furthermore, these theories predict an hydrostatic stress distribution in a crack tip different from classical plasticity crack. Therefore, with regard to diffusion results from Sofronis, McMeeking and Krom, it could represent a breakthrough [98].

Oudriss et al. [57] have found that $N_T$ decreases with grain size in polycrystalline nickel. As a first approximation they assumed that $N_T$ is due to geometrically necessary dislocations (GND), because the density of GND decreased as the grain size increased. But the difference between experimental $N_T$ and calculated $N_T^{GND}$ indicates that vacancies played a crucial role in trapping.

Dislocations are not immobile defects and, additionally, an hydrogen enhanced mobility has been found, establishing the HELP theory. From the previously defined transport model, Dadfarnia et al. [105] have implemented the mobility of dislocations by means of a drift term consisting of an hydrogen flux associated with mobile dislocations. This term allows to include dislocation mobility in transport models but does not consider how this mobility is hydrogen enhanced.

Moreover, Zhang et al. [47] found by way of quantum and molecular mechanics simulations that dislocations and stacking faults can promote the so-called “pipe diffusion” creating short-circuits for hydrogen.

*5.4.3. Non equilibrium*

Another option is to consider the influence of strain rate but assuming the formulation of McNabb and Foster [106], like in the simulation made by Kanayama et al. [107]. In this review, however, the development of Krom and Baker [52] is followed where the parameters are dimensionally consistent.

A general expression for $\partial C_T/\partial t$ must be found when Oriani's equilibrium is not satisfied. The variation of concentration in traps can be expressed as the total jumps from L to T minus the total jumps from T to L. Depending on the asymmetric transition rate, it can be expressed:

$$\frac{\partial C_\mathrm{T}}{\partial t} = C_\mathrm{L}\Gamma_{\mathrm{L}\to\mathrm{T}} - C_\mathrm{T}\Gamma_{\mathrm{T}\to\mathrm{L}}. \tag{54}$$

Krom and Bakker assume that the total number of interstitial sites is much greater than the total number of traps $N_L \gg N_T$ and, additionally, that there is a low occupancy $\theta_L \ll 1$, resulting in:

$$\frac{\partial C_\mathrm{T}}{\partial t} = \Omega_{\mathrm{L}\to\mathrm{T}}\theta_\mathrm{L}N_\mathrm{T}(1-\theta_\mathrm{T}) - \Omega_{\mathrm{T}\to\mathrm{L}}C_\mathrm{T}. \tag{55}$$

It is worth mentioning that, when traps can be assumed as irreversible because they represent deep potential wells, i.e. $E_{T\to L}$ is very high, then $\Omega_{T\to L} \approx 0$. Therefore, once these traps are saturated during diffusion, transport equations are independent of $C_T$.

In equilibrium, $\partial C_T/\partial t = 0$, representing a relationship between the parameters:

$$\frac{\Omega_{L\to T}}{\Omega_{T\to L}} = \frac{\theta_T}{\theta_L(1-\theta_T)} = K_T. \tag{56}$$

This means that Oriani's equilibrium is a particular case of the more general kinetic formulation.

Local equilibrium is usually considered in diffusion models due to its numerical simplicity, nonetheless this assumption is not valid when changes in lattice hydrogen concentrations are so fast that trapped hydrogen is not able to achieve the condition represented in (55) [89]. Oriani's hypothesis must be carefully held when kinetics might predominate, especially when defects with high binding energy exist [89,108] or in thermal desorption processes [109].

## 6. Coupled diffusion

The modelling of hydrogen damage and the discussion between localized plasticity and decohesion are beyond the scope of this review. However, it is essential to bear in mind that transport phenomena are determined by the stress-strain state. This

can also be observed in a multiscale approach: at mircostructural level, the crystal lattice is modified due to stress fields and therefore the energy states and microscopic interaction forces drift the diffusion; at continuous level, thermodynamic variables that phenomenologically describe transport are influenced by the elasticity and plasticity.

Based on the theoretical framework developed by Coleman and Noll [110], some authors [90,91] define the influence of mass transport in continuum mechanics through some internal state variables. Energy balance and entropy imbalance will lead to dissipation expressions for describing the evolution of the system in a thermodynamically consistent way. However, here the coupling of diffusion is described with a simplified treatment: on one hand with the alteration of the chemical potential by distortion (see Section 4.4) and on the other by modifying the constitutive elasto-plastic equation introducing hydrogen concentration. In this sense, from advances Sofronis et al. [23,25,111–113] is usually considered a double effect of hydrogen:

### 6.1. Local softening

Increasing mobility of dislocations, hydrogen induces a softening. This results in a reduction in resistance to local plastic flow $\sigma_Y$ [111,112,114,115]

$$\sigma_Y = \sigma_0(c) F(\varepsilon_P). \tag{57}$$

where $F(\varepsilon_P)$ is the strain hardening function; $\sigma_0(c)$ the yield strength before hardening and with an hydrogen concentration $c$ (measured in H atoms per metal atom); and $\sigma_0 = \sigma_0(0)$ is the yield strength in the absence of hydrogen. Softening can be assumed linear with a parameter $\xi < 1$.

$$\sigma_0(c) = [(\xi - 1)c + 1]\sigma_0. \tag{58}$$

Notably, according to Sofronis et al., although plastic flow will always be microscopically reduced, it may be increased macroscopically so a hardening produced by hydrogen will be observed. Either behaviour depends on the stress level, temperature, surface damage due to the electrolytic charging, etc. [2,116–118]. Once again, consistency between scales is required.

### 6.2. Lattice dilatation

Hydrogen produces a lattice dilatation [25,111–113] which can be expressed by adding a term $D_{ij}^t$ to the total deformation rate tensor $D_{ij}$ (besides the plastic and elastic part):

$$D_{ij} = D_{ij}^e + D_{ij}^p + D_{ij}^t. \tag{59}$$

This term [25] can be written in terms of true strain $\varepsilon^t$ associated with that dilatation and the Kronecker delta $\delta_{ij}$:

$$D_{ij}^t = \frac{d\varepsilon^t}{dt}\delta_{ij}. \tag{60}$$

$\delta_{ij}$ is the Kronecker delta and $\dot{\varepsilon^t}$ is the deformation due to expansion. However, the usual expression [119] relates dilatational engineering strain $e_{vol}^t$, i.e. volumetric true strain, with concentrations $c$ and $c_0$, local and initial respectively, present in the metal (measured in H atoms per metal atom):

$$e_{vol}^t = (c - c_0)\frac{\Delta v}{\Omega}. \tag{61}$$

Possible hydride formation of hydrides has not been considered here. In addition, $\Delta v$ is the volume change for each introduced hydrogen atom (related to the partial molar volume: $\Delta v = V_H/N_A$, being $N_A$ Avogadro's number) and $\Omega$ is the mean volume $\Omega$ of a metal atom. This engineering volumetric strain $e_{vol}^t$ needs to be transformed in a linear true strain. Considering that dilatation produces an equal strain in the three principal directions, it is finally obtained:

$$D_{ij}^t = \frac{d}{dt}\left\{ \ln\left[1 + \frac{(c - c_0)}{3}\frac{\Delta v}{\Omega}\right]\right\}\delta_{ij}. \tag{62}$$

Zhang and Hack [93] discuss the situations where deformation is not only dilatational but there is a tetragonal distortion.

Considering this double hydrogen effect, and substituting the found expressions for $D_{ij}^p$ and $D_{ij}^t$ depending on concentration, the constitutive equation obtained is of the form:

$$\dot{\sigma} = f\left(D_{ij}\right). \tag{63}$$

Summing up, hydrogen transport depends on the equivalent plastic strain and the hydrostatic stress, which leads to claim that it is a coupled problem and its resolution should be an iterative process.

Coupled elasto-plastic equations (Eqs. (57) and (62)) include total concentration, i.e. hydrogen in lattice sites as well as trapped hydrogen. However, dilatation would not be the same in both sites and local softening mainly depends on hydrogen interaction with dislocations. Therefore an atomistic approach should enrich continuum elaso-plastic equations in order to discriminate coupling effects depending on whether hydrogen is in lattice sites or in defects.

Apart from hydrogen transport, fracture modelling using Cohesive Zone Models [120] also will use a hydrogen concentration modifying the parameters of the constitutive law, particularly the traction-separation law [61].

There is also an effect of hydrogen on dislocation nucleation [121] so ductile continuum damage models, e.g. Gurson model [122], might incorporate hydrogen concentration as a parameter [123].

Although these numerical models pay attention to diffusion in a crack tip within the context of fracture mechanics, comparison with experimental values is very problematic because it is not easy to measure a hydrogen concentration so localized. Promising methods are Secondary Ion Mass Spectrometry (SIMS) [124,125] and Micro-Print Technique [126].

## 7. Conclusions

Although hydrogen embrittlement in different materials has been documented and studied for a century, mechanisms by which it is produced are not yet entirely clear. Therefore, the hydrogen-metal interaction should be best described to elucidate these mechanisms and to predict possible failures.

The emerging technologies of hydrogen as an energy carrier require a qualitative and quantitative modelling in order to optimize the use of fuel cells and hydrogen storage vessels. In this context, combining modelling with experimental results will allow the selection of less susceptible alloys.

The present review has tried to show how diffusion is a random phenomenon at the atomic level when the thermodynamic potentials are uniform. Nevertheless, when there is an imposed tensional field, for example, or when the crystal lattice defects act as retention sites, the usual Fick laws must be modified.

In that approach the gradient of the chemical potential is considered as the driving force of diffusion. Its expression depending on the hydrogen occupation can be found through the partition function in the context of statistical mechanics. Fermi-Dirac distribution and degeneracy of the existing defects can be also used to find that expression.

Moreover, thermodynamic studies of stressed solids define how the chemical potential is modified by a given stress state in the metallic bulk. It will be essential in the future to describe better the anisotropic distortion of the cells.

Finally, mass balance equations representing the modified Fick's second law are obtained. Each model must consider a kinetic relationship between traps and interstitial sites so all models that are reviewed here are called two-level models. When Oriani's equilibrium is not applicable, the generic kinetic formulation of McNabb and Foster must be used.

As an introduction to coupled diffusion, a double hydrogen effect is noted: local softening and lattice dilatation. Although constitutive equations are not developed in the context of the continuum mechanics, this approach can be interesting for a finite element simulation of a component or specimen subjected to both hydrogen environment and a certain stress state.

To sum up, hydrogen transport at continuous level is a multidisciplinary and multiscale phenomenon. In this review, it has been tried to recapitulate the underlying physics fundamentals and to translate them into some constitutive equations that will allow a more accurate and consistent numerical simulation.

## Acknowledgements

The authors are grateful for the funding received from project MCI Ref: MAT2014-58738-C3-2-R.

## References

[1] A. Barnoush, Hydrogen Embrittlement, Saarland University, 2011.
[2] J. Hirth, Effects of hydrogen on the properties of iron and steel, Metall. Trans. A 11 (1980) 861–890.
[3] R.P. Gangloff, B.P. Somerday, Gaseous Hydrogen Embrittlement of Materials in Energy Technologies: Mechanisms, Modelling and Future Developments, Elsevier, 2012.
[4] R.A. Oriani, Hydrogen embrittlement of steels, Annu. Rev. Mater. Sci. 8 (1978) 327–357.
[5] D. Delafosse, T. Magnin, Hydrogen induced plasticity in stress corrosion cracking of engineering systems, Eng. Fract. Mech. 68 (2001) 693–729.
[6] S. Lynch, Progress Towards Understanding Mechanisms of Hydrogen Embrittlement and Stress Corrosion Cracking, CORROSION 2007: NACE International, 2007.
[7] I. Bernstein, The role of hydrogen in the embrittlement of iron and steel, Mater. Sci. Eng. 6 (1970) 1–19.
[8] M. Hadianfard, Failure in a high pressure feeding line of an oil refinery due to hydrogen effect, Eng. Fail. Anal. 17 (2010) 873–881.
[9] A.H.S. Bueno, E.D. Moreira, J.A.C.P. Gomes, Evaluation of stress corrosion cracking and hydrogen embrittlement in an API grade steel, Eng. Fail. Anal. 36 (2014) 423–431.
[10] D. Hardie, E.A. Charles, A.H. Lopez, Hydrogen embrittlement of high strength pipeline steels, Corros. Sci. 48 (2006) 4378–4385.
[11] S.A. Shipilov, I. Le May, Structural integrity of aging buried pipelines having cathodic protection, Eng. Fail. Anal. 13 (2006) 1159–1176.
[12] Z. Zhenqian, T. Zhiling, Y. Chun, L. Shuangping, Failure analysis of vessel propeller bolts under fastening stress and cathode protection environment, Eng. Fail. Anal. 57 (2015) 129–136.
[13] G. Tanner, Hydrogen embrittlement failure of socket head cap screws, ASM International, Handbook of Case Histories in Failure Analysis, 1 1992, pp. 332–334.
[14] R.K. Dayal, N. Parvathavarthini. Hydrogen embrittlement in power plant steels, Sadhana 28 431–451.
[15] J.M. Pardal, S.S.M. Tavares, B.A.R.S. Barbosa, F.B. Mainier, J.S. Corte, J.P. Pardal, Investigation of hydrogen embrittlement failure in a steam separator by field metallography, Eng. Fail. Anal. 35 (2013) 46–53.
[16] L. Zhou, Progress and problems in hydrogen storage methods, Renew. Sust. Energ. Rev. 9 (2005) 395–408.

[17] T. Boellinghaus, K. Holtappels, G.W. Mair, T. Grunewald, Explosion of iron hydrogen storage containers – investigations from 120 years ago revisited, Eng. Fail. Anal. 43 (2014) 47–62.
[18] R.P. Jewett, R. Walter, W. Chandler, R. Frohmberg, Hydrogen Environment Embrittlement of Metals, 1973.
[19] ANSI/CSA CHMC 1-, Test Method for Evaluating Material Compatibility in Compressed Hydrogen Applications – Phase I – Metals, 2014.
[20] E.A. Steigerwald, F.W. Schaller, A.R. Troiano, The role of stress in hydrogen induced delayed failureJournal Name Trans. Metall. Soc. AIME Vol. 218 (1960) 832–841 Journal Volume. Other Information: Orig. Receipt Date: 31-DEC-61. Medium: X; Size: Pages.
[21] R.A. Oriani, P.H. Josephic, Equilibrium aspects of hydrogen-induced cracking of steels, Acta Metall. 22 (1974) 1065–1074.
[22] W.W. Gerberich, Y.T. Chen, Hydrogen-controlled cracking—an approach to threshold stress intensity, Metall. Trans. A 6 (1975) 271–278.
[23] H.K. Birnbaum, P. Sofronis, Hydrogen-enhanced localized plasticity—a mechanism for hydrogen-related fracture, Mater. Sci. Eng. A 176 (1994) 191–202.
[24] J. Lufrano, P. Sofronis, H.K. Birnbaum, Modeling of hydrogen transport and elastically accommodated hydride formation near a crack tip, J. Mech. Phys. Solids 44 (1996) 179–205.
[25] J. Lufrano, P. Sofronis, H.K. Birnbaum, Elastoplastically accommodated hydride formation and embrittlement, J. Mech. Phys. Solids 46 (1998) 1497–1520.
[26] C.V. Owen, T.E. Scott, Relation between hydrogen embrittlement and formation of hydride in group V transition-metals, Metall. Trans. 3 (1972) 1715 (-&).
[27] M.F. Horstemeyer, Multiscale modeling: a review, Practical Aspects of Computational Chemistry, Springer 2010, pp. 87–135.
[28] M.N. Risto, From atomistic simulation towards multiscale modelling of materials, J. Phys. Condens. Matter 14 (2002) 2859.
[29] A.M. Stoneham, Non- classical diffusion processes, J. Nucl. Mater. 69 (1978) 109–116.
[30] A.T. Paxton, From quantum mechanics to physical metallurgy of steels, Mater. Sci. Technol. 30 (2014) 1063–1070.
[31] A. Stoneham, Theory of the diffusion of hydrogen in metals, Ber. Bunsenges. Phys. Chem. 76 (1972) 816–823.
[32] A. Stoneham, Quantum theory of diffusion: temperature dependence of diffusion of light interstitials in Debye solids, J. Phys. F: Met. Phys. 2 (1972) 417.
[33] K. Yu, M.I. Klinger, Theory of quantum diffusion of atoms in crystals, J. Phys. C Solid State Phys. 7 (1974) 2791.
[34] R. Kirchheim, Monte-Carlo simulations of interstitial diffusion and trapping—I. One type of traps and dislocations, Acta Metall. 35 (1987) 271–280.
[35] R. Kirchheim, U. Stolz, Monte-Carlo simulations of interstitial diffusion and trapping—II. Amorphous metals, Acta Metall. 35 (1987) 281–291.
[36] J.M. Bockris, P. Subramanyan, The equivalent pressure of molecular hydrogen in cavities within metals in terms of the overpotential developed during the evolution of hydrogen, Electrochim. Acta 16 (1971) 2169–2179.
[37] W. Beck, J.M. Bockris, J. McBreen, L. Nanis, Hydrogen permeation in metals as a function of stress, temperature and dissolved hydrogen concentration, Proceedings of the Royal Society of London A: Mathematical, Physical and Engineering Sciences, vol. 290, The Royal Society 1966, pp. 220–235.
[38] Q. Liu, A.D. Atrens, Z. Shi, K. Verbeken, A. Atrens, Determination of the hydrogen fugacity during electrolytic charging of steel, Corros. Sci. 87 (2014) 239–258.
[39] H. Mehrer, N.A. Stolwijk, Heroes and Highlights in the History of Diffusion, 2009.
[40] A. Einstein, On the theory of the Brownian movement, Ann. Phys. 4 (1906) 371–381.
[41] E.F. Schubert, Doping in III–V Semiconductors, Cambridge University Press, 2005.
[42] J. Crank, The Mathematics of Diffusion, Oxford university press, 1979.
[43] A.R. Altenberger, On the theory of generalized diffusion processes in many-particle systems, Physica A: Statistical Mechanics and its Applications 92 (1978) 391–409.
[44] C. Tsallis, D.J. Bukman, Anomalous diffusion in the presence of external forces: exact time-dependent solutions and their thermostatistical basis, Phys. Rev. E 54 (1996) R2197.
[45] M.S. Daw, M.I. Baskes, Semiempirical, quantum mechanical calculation of hydrogen embrittlement in metals, Phys. Rev. Lett. 50 (1983) 1285.
[46] M.S. Daw, M.I. Baskes, Embedded-atom method: derivation and application to impurities, surfaces, and other defects in metals, Phys. Rev. B 29 (1984) 6443.
[47] X. Zhang, Q. Peng, G. Lu, Self-consistent embedding quantum mechanics/molecular mechanics method with applications to metals, Phys. Rev. B 82 (2010) 134120.
[48] Y. Zhao, G. Lu, QM/MM study of dislocation—hydrogen/helium interactions in α-Fe, Model. Simul. Mater. Sci. Eng. 19 (2011) 065004.
[49] H. Grabert, H. Wipf, Tunneling of hydrogen in metals, in: U. Rössler (Ed.), Festkörperprobleme 30, vol. 30, Springer, Berlin Heidelberg 1990, pp. 1–23.
[50] I.H. Katzarov, D.L. Pashov, A.T. Paxton, Fully quantum mechanical calculation of the diffusivity of hydrogen in iron using the tight-binding approximation and path integral theory, Phys. Rev. B 88 (2013) 054107.
[51] G.M. Pressouyre, Trap theory of hydrogen embrittlement, Acta Metall. 28 (1980) 895–911.
[52] A.M. Krom, A. Bakker, Hydrogen trapping models in steel, Metall. Mater. Trans. B Process Metall. Mater. Process. Sci. 31 (2000) 1475–1482.
[53] K. Kehr, Theory of the diffusion of hydrogen in metals, Hydrogen in Metals I, Springer 1978, pp. 197–226.
[54] R. Kirchheim, Solubility, diffusivity and trapping of hydrogen in dilute alloys. Deformed and amorphous metals—II, Acta Metall. 30 (1982) 1069–1078.
[55] M. Nagumo, K. Takai, N. Okuda, Nature of hydrogen trapping sites in steels induced by plastic deformation, J. Alloys Compd. 293 (1999) 310–316.
[56] K. Takai, G. Yamauchi, M. Nakamura, M. Nagumo, Hydrogen trapping characteristics of cold-drawn pure iron and eutectoid steel evaluated by thermal desorption spectrometry, Journal of the Japan Institute of Metals (Japan) 62 (1998) 267–275.
[57] A. Oudriss, J. Creus, J. Bouhattate, E. Conforto, C. Berziou, C. Savall, X. Feaugas, Grain size and grain-boundary effects on diffusion and trapping of hydrogen in pure nickel, Acta Mater. 60 (2012) 6814–6828.
[58] I. Maroef, D. Olson, M. Eberhart, G. Edwards, Hydrogen trapping in ferritic steel weld metal, Int. Mater. Rev. 47 (2002) 191–223.
[59] M. Wen, X.-J. Xu, S. Fukuyama, K. Yokogawa, Embedded-atom-method functions for the body-centered-cubic iron and hydrogen, J. Mater. Res. 16 (2001) 3496–3502.
[60] A. Oudriss, J. Creus, J. Bouhattate, C. Savall, B. Peraudeau, X. Feaugas, The diffusion and trapping of hydrogen along the grain boundaries in polycrystalline nickel, Scr. Mater. 66 (2012) 37–40.
[61] A. Alvaro, I. Thue Jensen, N. Kheradmand, O.M. Løvvik, V. Olden, Hydrogen embrittlement in nickel, visited by first principles modeling, cohesive zone simulation and nanomechanical testing, Int. J. Hydrog. Energy 40 (2015) 16892–16900.
[62] E. Wimmer, W. Wolf, J. Sticht, P. Saxe, C.B. Geller, R. Najafabadi, G.A. Young, Temperature-dependent diffusion coefficients from ab initio computations: hydrogen, deuterium, and tritium in nickel, Phys. Rev. B 77 (2008) 134305.
[63] G. Schaumann, J. Völki, G. Alefeld, The diffusion coefficients of hydrogen and deuterium in vanadium, niobium, and tantalum by Gorsky-effect measurements, Phys. Status Solidi B 42 (1970) 401–413.
[64] A. Ferro, Theory of diffusion constants in interstitial solid solutions of bcc metals, J. Appl. Phys. 28 (1957) 895–900.
[65] J. Toribio, V. Kharin, A generalised model of hydrogen diffusion in metals with multiple trap types, Philos. Mag. (2015) 1–23.
[66] P. Sofronis, R.M. McMeeking, Numerical analysis of hydrogen transport near a blunting crack tip, J. Mech. Phys. Solids 37 (1989) 317–350.
[67] R.B. Bird, W.E. Stewart, E.N. Lightfoot, Transport Phenomena, Wiley, 2007.
[68] A. Gorban, H. Sargsyan, H. Wahab, Quasichemical models of multicomponent nonlinear diffusion, Mathematical Modelling of Natural Phenomena 6 (2011) 184–262.
[69] L. Onsager, Reciprocal relations in irreversible processes, I, Phys. Rev. 37 (1931) 405.
[70] L. Onsager, Reciprocal relations in irreversible processes, II, Phys. Rev. 38 (1931) 2265.
[71] J. Wijmans, R. Baker, The solution-diffusion model: a review, J. Membr. Sci. 107 (1995) 1–21.
[72] M. Danielewski, B. Wierzba, Thermodynamically consistent bi-velocity mass transport phenomenology, Acta Mater. 58 (2010) 6717–6727.
[73] R.M. Neumann, Entropic approach to Brownian movement, Am. J. Phys. 48 (1980) 354–357.
[74] G. Venturini, K. Wang, I. Romero, M. Ariza, M. Ortiz, Atomistic long-term simulation of heat and mass transport, J. Mech. Phys. Solids 73 (2014) 242–268.
[75] Y. Fukai, The Metal-Hydrogen System: Basic Bulk Properties, Springer Science & Business Media, 2006.
[76] J. Lumsden, Thermodynamics of Alloys, Inst. of Metals, 1952.
[77] C.H.P. Lupis, J.F. Elliott, Prediction of enthalpy and entropy interaction coefficients by the “central atoms” theory, Acta Metall. 15 (1967) 265–276.
[78] R.B. McLellan, Invited review: thermodynamics of solid solutions, Mater. Sci. Eng. 9 (1972) 121–140.

[79] E. Guggenheim, M. McGlashan, Statistical mechanics of regular mixtures, Proceedings of the Royal Society of London, A: Mathematical, Physical and Engineering Sciences, vol. 206, The Royal Society 1951, pp. 335–353.
[80] K. Alex, R.B. McLellan, A zeroth order mixing treatment of interstitial solid solutions, J. Phys. Chem. Solids 31 (1970) 2751–2753.
[81] R.B. McLellan, W.W. Dunn, A quasi-chemical treatment of interstitial solid solutions: it application to carbon austenite, J. Phys. Chem. Solids 30 (1969) 2631–2637.
[82] O.B. Christensen, P. Stoltze, K.W. Jacobsen, J.K. Nrskov, Effective-medium calculations for hydrogen in Ni, Pd, and Pt, Phys. Rev. B 41 (1990) 12413–12423.
[83] J.R. Lacher, The statistics of the hydrogen-palladium system, Math. Proc. Camb. Philos. Soc. 33 (1937) 518–523.
[84] J.R. Lacher, A theoretical formula for the solubility of hydrogen in palladium, Proceedings of the Royal Society of London, Series A, Mathematical and Physical Sciences, 161 1937, pp. 525–545.
[85] R. Kirchheim, Hydrogen solubility and diffusivity in defective and amorphous metals, Prog. Mater. Sci. 32 (1988) 261–325.
[86] D.L. Anderson, Theory of the Earth, Blackwell scientific publications, 1989.
[87] P. Hao, Y. Fang, J. Sun, G.I. Csonka, P.H.T. Philipsen, J.P. Perdew, Lattice constants from semilocal density functionals with zero-point phonon correction, Phys. Rev. B 85 (2012) 014111.
[88] D. Jiang, E.A. Carter, First principles assessment of ideal fracture energies of materials with mobile impurities: implications for hydrogen embrittlement of metals, Acta Mater. 52 (2004) 4801–4807.
[89] R.A. Oriani, The diffusion and trapping of hydrogen in steel, Acta Metall. 18 (1970) 147–157.
[90] C.V. Di Leo, L. Anand, Hydrogen in metals: a coupled theory for species diffusion and large elastic–plastic deformations, Int. J. Plast. 43 (2013) 42–69.
[91] M.E. Gurtin, E. Fried, L. Anand, The Mechanics and Thermodynamics of Continua, Cambridge University Press, 2010.
[92] A.G. McLellan, Non-hydrostatic Thermodynamics of Chemical Systems, 1970.
[93] T.-Y. Zhang, J.E. Hack, The equilibrium concentration of hydrogen atoms ahead of a mixed mode I–mode III crack tip in single crystal iron, Metall. Mater. Trans. A 30 (1999) 155–159.
[94] I.M. Robertson, The effect of hydrogen on dislocation dynamics, Eng. Fract. Mech. 68 (2001) 671–692.
[95] P. Sofronis, H.K. Birnbaum, Mechanics of the hydrogendashdislocationdashimpurity interactions—I. Increasing shear modulus, J. Mech. Phys. Solids 43 (1995) 49–90.
[96] J.B. Leblond, D. Dubois, A general mathematical description of hydrogen diffusion in steels—II. Numerical study of permeation and determination of trapping parameters, Acta Metall. 31 (1983) 1471–1478.
[97] J.B. Leblond, D. Dubois, A general mathematical description of hydrogen diffusion in steels—I. Derivation of diffusion equations from boltzmann-type transport equations, Acta Metall. 31 (1983) 1459–1469.
[98] A. Turnbull. Perspectives on hydrogen uptake, diffusion and trapping, Int. J. Hydrog. Energy.
[99] H. Van Leeuwen, The kinetics of hydrogen embrittlement: a quantitative diffusion model, Eng. Fract. Mech. 6 (1974) 141–161.
[100] A. Krom, R. Koers, A. Bakker, Hydrogen transport near a blunting crack tip, J. Mech. Phys. Solids 47 (1999) 971–992.
[101] W. Dietzel, M. Pfuff, G.G. Juilfs, Hydrogen permeation in plastically deformed steel membranes, Mater. Sci. 42 (2006) 78–84.
[102] G. Juilfs, Das Diffusionsverhalten von Wasserstoff in einem niedriglegierten Stahl unter Berücksichtigung des Verformungsgrades, GRIN Verlag, 2002.
[103] A.J. Kumnick, H.H. Johnson, Deep trapping states for hydrogen in deformed iron, Acta Metall. 28 (1980) 33–39.
[104] P. Sofronis, Y. Liang, N. Aravas, Hydrogen induced shear localization of the plastic flow in metals and alloys, Eur. J. Mech. A. Solids 20 (2001) 857–872.
[105] M. Dadfarnia, M.L. Martin, A. Nagao, P. Sofronis, I.M. Robertson, Modeling hydrogen transport by dislocations, J. Mech. Phys. Solids 78 (2015) 511–525.
[106] A. McNabb, P.K. Foster, A new analysis of the diffusion of hydrogen in iron and ferritic steels, Trans. Metall. Soc. AIME 227 (1963) 618–627.
[107] H. Kanayama, S. Ndong-Mefane, M. Ogino, R. Miresmaeili, Reconsideration of the hydrogen diffusion model using the mcnabb-foster formulation, Memoirs of the Faculty of Engineering, Kyushu University 69 (2009) 149–161.
[108] A. Thompson, I. Bernstein, R. Swanson, Stress Corrosion Cracking of Wrought and P/M High Strength Aluminum Alloys, DTIC Document, 1982.
[109] K.-i. Ebihara, H. Kaburaki, T. Suzudo, K. Takai, A numerical study on the validity of the local equilibrium hypothesis in modeling hydrogen thermal desorption spectra, ISIJ Int. 49 (2009) 1907–1913.
[110] B. Coleman, W. Noll, The thermodynamics of elastic materials with heat conduction and viscosity, Arch. Ration. Mech. Anal. 13 (1963) 167–178.
[111] Y. Liang, P. Sofronis, Toward a phenomenological description of hydrogen-induced decohesion at particle/matrix interfaces, J. Mech. Phys. Solids 51 (2003) 1509–1531.
[112] Y. Liang, P. Sofronis, N. Aravas, On the effect of hydrogen on plastic instabilities in metals, Acta Mater. 51 (2003) 2717–2730.
[113] A. Taha, P. Sofronis, A micromechanics approach to the study of hydrogen transport and embrittlement, Eng. Fract. Mech. 68 (2001) 803–837.
[114] H. Kotake, R. Matsumoto, S. Taketomi, N. Miyazaki, Transient hydrogen diffusion analyses coupled with crack-tip plasticity under cyclic loading, Int. J. Press. Vessel. Pip. 85 (2008) 540–549.
[115] R. Miresmaeili, M. Ogino, T. Nakagawa, H. Kanayama, A coupled elastoplastic-transient hydrogen diffusion analysis to simulate the onset of necking in tension by using the finite element method, Int. J. Hydrog. Energy 35 (2010) 1506–1514.
[116] R.A. Oriani, The hardening and softening induced by hydrogen in carbon steels, in: R.M. Latanision, J.R. Pickens (Eds.), Atomistics of Fracture, Springer US 1983, pp. 795–798.
[117] H. Kimura, H. Matsui, Mechanism of hydrogen-induced softening and hardening in iron, Scr. Metall. 21 (1987) 319–324.
[118] H. Matsui, H. Kimura, S. Moriya, The effect of hydrogen on the mechanical properties of high purity iron I. Softening and hardening of high purity iron by hydrogen charging during tensile deformation, Mater. Sci. Eng. 40 (1979) 207–216.
[119] H. Peisl, Lattice strains due to hydrogen in metals, Hydrogen in Metals I, Springer 1978, pp. 53–74.
[120] V. Olden, C. Thaulow, R. Johnsen, E. Østby, Cohesive zone modeling of hydrogen-induced stress cracking in 25% Cr duplex stainless steel, Scr. Mater. 57 (2007) 615–618.
[121] A. Barnoush, H. Vehoff, Recent developments in the study of hydrogen embrittlement: hydrogen effect on dislocation nucleation, Acta Mater. 58 (2010) 5274–5285.
[122] A.L. Gurson, Continuum theory of ductile rupture by void nucleation and growth: part I—yield criteria and flow rules for porous ductile media, J. Eng. Mater. Technol. 99 (1977) 2–15.
[123] M. Grange, J. Besson, E. Andrieu, An anisotropic Gurson type model to represent the ductile rupture of hydrided Zircaloy-4 sheets, Int. J. Fract. 105 (2000) 273–293.
[124] A.M. Brass, J. Chene, A. Boutry-Forveille, Measurements of deuterium and tritium concentration enhancement at the crack tip of high strength steels, Corros. Sci. 38 (1996) 569–585.
[125] S.X. Mao, M. Li, Mechanics and thermodynamics on the stress and hydrogen interaction in crack tip stress corrosion: experiment and theory, J. Mech. Phys. Solids 46 (1998) 1125–1137.
[126] K. Kawamoto, Y. Oda, H. Noguchi, H. Fujii, T. Izumi, G. Itoh, Investigation of local hydrogen distribution around fatigue crack tip of a type 304 stainless steel with secondary ion mass spectrometry and hydrogen micro-print technique, J. Mech. Phys. Solids 3 (2009) 898–909.